AIMS Geosciences

AIMS Geosciences, 5(4): 921–939.
DOI: 10.3934/geosci.2019.4.921
Received: 19 February 2019
Accepted: 17 October 2019
Published: 12 November 2019

http://www.aimspress.com/journal/geosciences

Research article

Unsaturated behavior of excavations in residual soil at the Auburn University National Geotechnical Experimentation Site

Richard E. Burrage[1] and J. Brian Anderson[2,*]

[1] Richard Burrage, Inc., 675 Knollcrest Dr. NE., Concord, NC 28025, USA
[2] Civil Engineering, Auburn University, 238 Harbert Engineering Center, Auburn University, AL 36849, USA

*** Correspondence:** Email: jbanders@auburn.edu; Tel: +13348447373; Fax: +13348446290.

Abstract: Two excavations were instrumented at the Auburn National Geotechnical Experimentation Site (NGES) in Opelika, AL. The excavations were constructed approximately 6 m deep × 30 m long with a vertical face. The primary goal of this experiment was to determine the boundary conditions that resulted in failure of the excavation. In doing so, conclusions were drawn regarding the accuracy of common laboratory test methods for estimating the strength properties of residual soil.

The instrumentation plan was designed to monitor real-time pore water pressures (positive and negative) surrounding the excavation throughout the course of each 1-year test period. Time-lapse cameras were used to identify when failures occurred, and the approximate geometry of the failure planes. Undisturbed soil samples were taken during the subsurface exploration and used in conjunction with previous soil test results to accurately define the material properties and layering based on common laboratory test methods. In addition to common laboratory tests, unsaturated triaxial tests were also conducted, and soil-water characteristic curves were measured to further define the unsaturated properties of the soil.

In both excavations, failure was observed along a similar plane, which began at the bottom of the excavation, and propagated to the surface (approximately 2 m behind the face of the excavation) along existing tension cracks that developed during the construction of the excavation. Based on these results, recommendations are provided as related to the most appropriate test methods for determining the strength properties of residual soil for use in geotechnical design.

Keywords: residual soil; unsaturated soil; excavations; full scale testing

1. Introduction

Residual soil behavior can be difficult to predict using existing geotechnical formulas, because it exhibits properties that are not common to transported soils. These unique properties are mainly influenced by the fabric of the soil, and the cohesive nature of undisturbed residual soils that remains from the weathering process of the parent rock. Because of these unique properties, residual soils do not fit in the typical categories of "sand" or "clay" when used in geotechnical design, but exhibit behaviors of both, along with some unique behavior not seen in most design methods. Classical engineering design methods usually assume that soil will behave as either sand ($c = 0$), or saturated clay ($\phi = 0$). However, because of the unique properties of residual soil, it is often considered to be a c-ϕ soil, having both frictional and cohesive properties. Several obstacles exist that need to be overcome before residual soil mechanics can be implemented into routine engineering practice:

- Residual soil strength properties can easily be mistaken for unsaturated strength properties.
- Unsaturated properties are volatile in nature and can change over time as the soil moisture conditions change which could result in failure.
- Common characterization methods are unable to differentiate the residual soil strength properties from the temporary effects of matric suction.

The main goal of this project was to learn more about the behavior of unsaturated residual soils, and to be able to apply this knowledge to classical engineering design methods to promote both efficiency and safety in design. Although substantial research has supported the theory that residual soil behaves as a c-ϕ soil (having both frictional and cohesive properties), there have been other case studies of residual soil slopes that have failed after being seemingly stable for long periods of time, causing researchers and practitioners to question whether or not the c-ϕ nature should be considered in designs that may need to withstand decades or even centuries. Furthermore, determining the strength parameters for design can be challenging, because many characterization methods are not able to differentiate the cohesion created by negative pore pressures from the residual soil cohesion, making it difficult to determine the strength parameters for use in long term designs. For these reasons, further research is needed to better understand the behavior of residual soil to enable the engineering community to be able to take advantage of residual strength properties without sacrificing safety. In this project, two excavations were constructed that would remain stable when unsaturated but would become unstable as the surrounding soil neared saturation so that failure was observed and monitored.

2. Instrumentation plan

The main goals of the instrumentation plan were to (1) determine the boundary conditions at failure for the test excavations, and (2) observe movement in the soil mass throughout the observation period. The instrumentation plan for this test included a combination of sensors that were connected to an automated data acquisition system to continually measure pore pressures for the excavation, as well as water levels in the bottom of the excavation, and changes in soil moisture content near the surface. Slope inclinometers were used to determine deflection over time, and time-lapse cameras were used to determine other site conditions at failure. Weather data was also collected at nearby weather stations (KALAAUBR4, and MTKGA1).

The instrumentation for the test excavations included soil matric potential (SMP) sensors, soil temperature sensors, soil piezometers (equipped with high air entry (HAE) filters to measure negative pore pressures), dielectric water content reflectometers (WCR), and an automated data acquisition system (DAQ). This instrumentation setup was designed to measure pore pressure and water content over long periods of time without having to perform maintenance on the sensors. To monitor movement in the soil mass, slope inclinometer casing was installed, and a slope inclinometer was used periodically to take measurements. Time-lapse cameras were also used to monitor the movement and failures of the soil mass, as well as to collect observational data on the conditions at failure, such as undermining of the excavation face, or standing water at the surface or in the bottom of the excavation. Instrumentation plans for the excavations along with the approximate dimensions of the test excavations and the instrumentation borehole locations are shown in Figures 1 and 2.

The first excavation included additional boreholes so that the pore pressure sensors were each installed in separate boreholes, and the depth of the borehole was made so that the sensors were located in the bottom (partially in contact with the residual soil). However, because the failure surface observed in Excavation #1 intersected the boreholes closest to the excavation, Excavation #2 was modified to minimize the number of boreholes within 2 meters of the excavation, therefore minimizing the disturbance of the soil in that region. It was determined that installing the sensors in re-compacted soils as shown in Figure 2 would not introduce significant error in the measurements, because the small diameter of the borehole would result in a relatively low fluctuation in pore pressure with respect to the soil surrounding the borehole (i.e. the pore pressure would equalize with the soil surrounding the borehole at each depth). This same concept is the basis for the Watermark sensor design, and the filter paper method for determining suction [1]. Also, to better see the site conditions at failure, a time lapse camera was installed for the second excavation to take photographs every hour. The approximate locations of the two test excavations are shown in Figure 3.

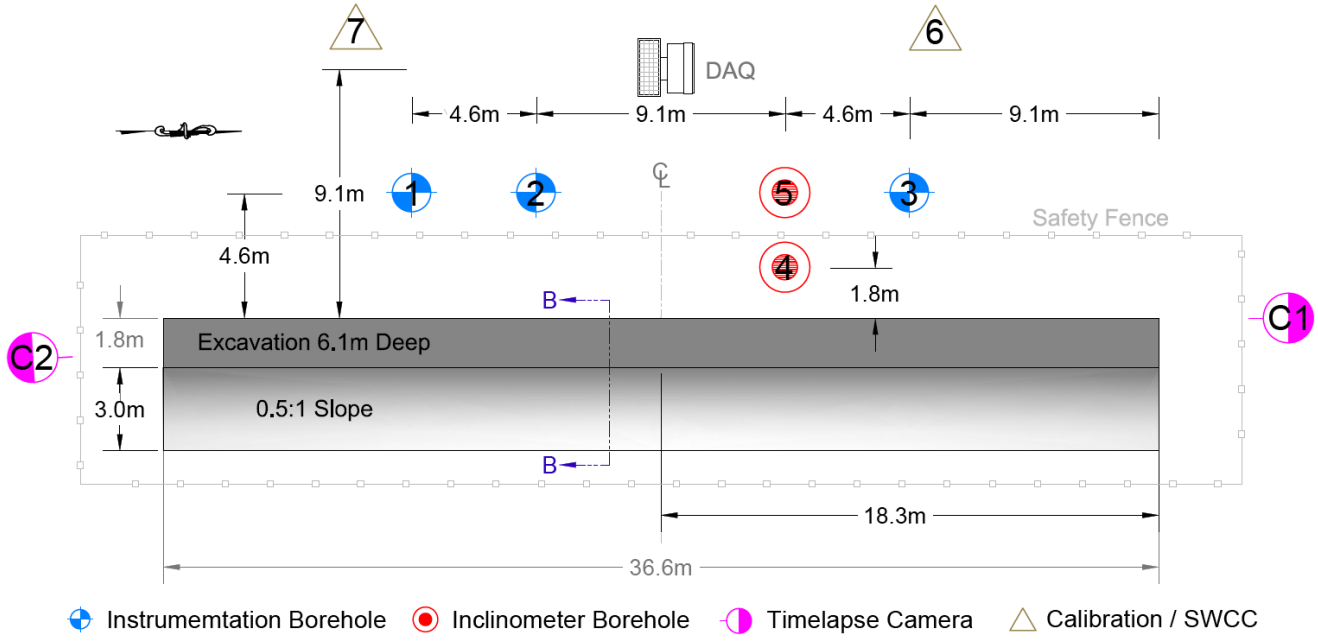

Figure 1. Excavation instrumentation plan.

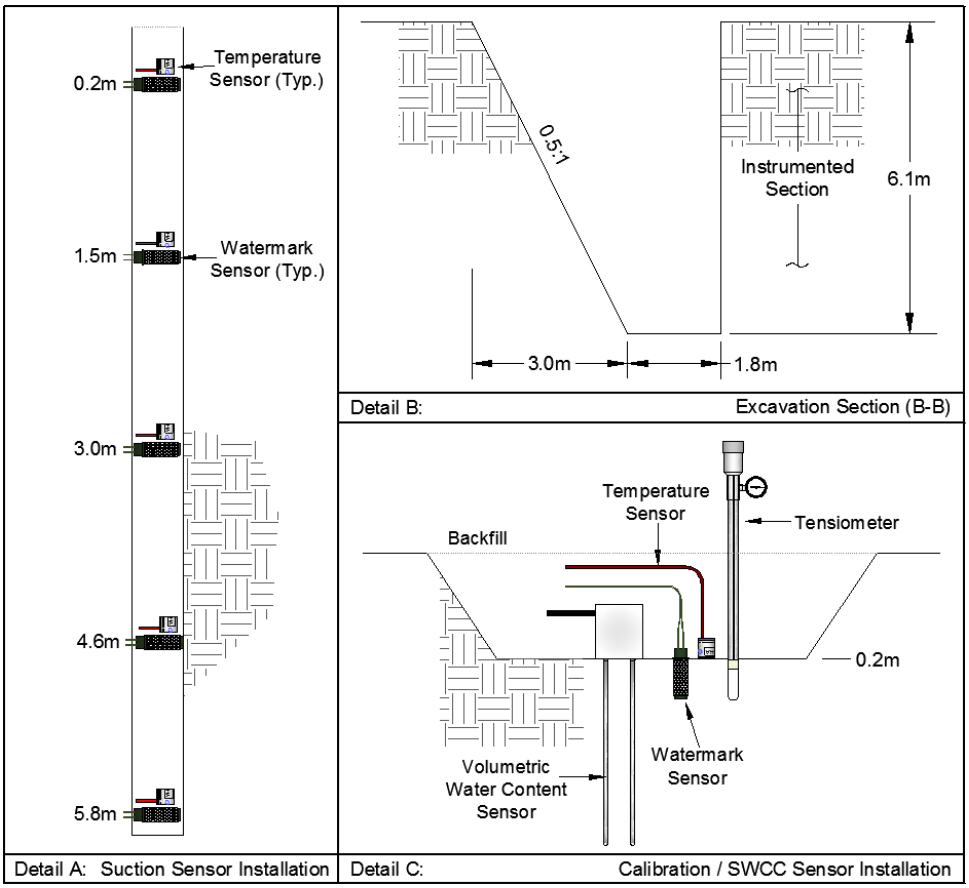

Figure 2. Excavation/instrumentation details.

Figure 3. NGES aerial with approximate excavation locations [2].

3. Site characterization

3.1. Insitu testing

The Auburn University NGES is located in the Southwest portion of the Piedmont region of the United States (32°35′39″ N, 85°17′50″ W). Previous researchers such as Vinson and Brown [3] have conducted a variety of insitu and laboratory tests at the Auburn NGES. Site specific testing in close proximity to the excavation was also performed to develop a stratigraphic profile of the site under the excavation location, and to retrieve samples for laboratory testing. Standard Penetration Tests (SPT) were performed in three instrumentation boreholes located on the West side of Excavation #2. Because the SPT is so widely used in the United States, it was performed in order to aid in future correlations of data. The geotechnical drill rig performing the SPT was also used to retrieve undisturbed samples in thin-wall samplers for further laboratory testing as presented in Section 3.2. Cone Penetration Tests (CPT) were also performed in close proximity to the location of the excavations to provide additional data for future comparisons of data. A summary of the CPT and SPT results is shown in Figure 4.

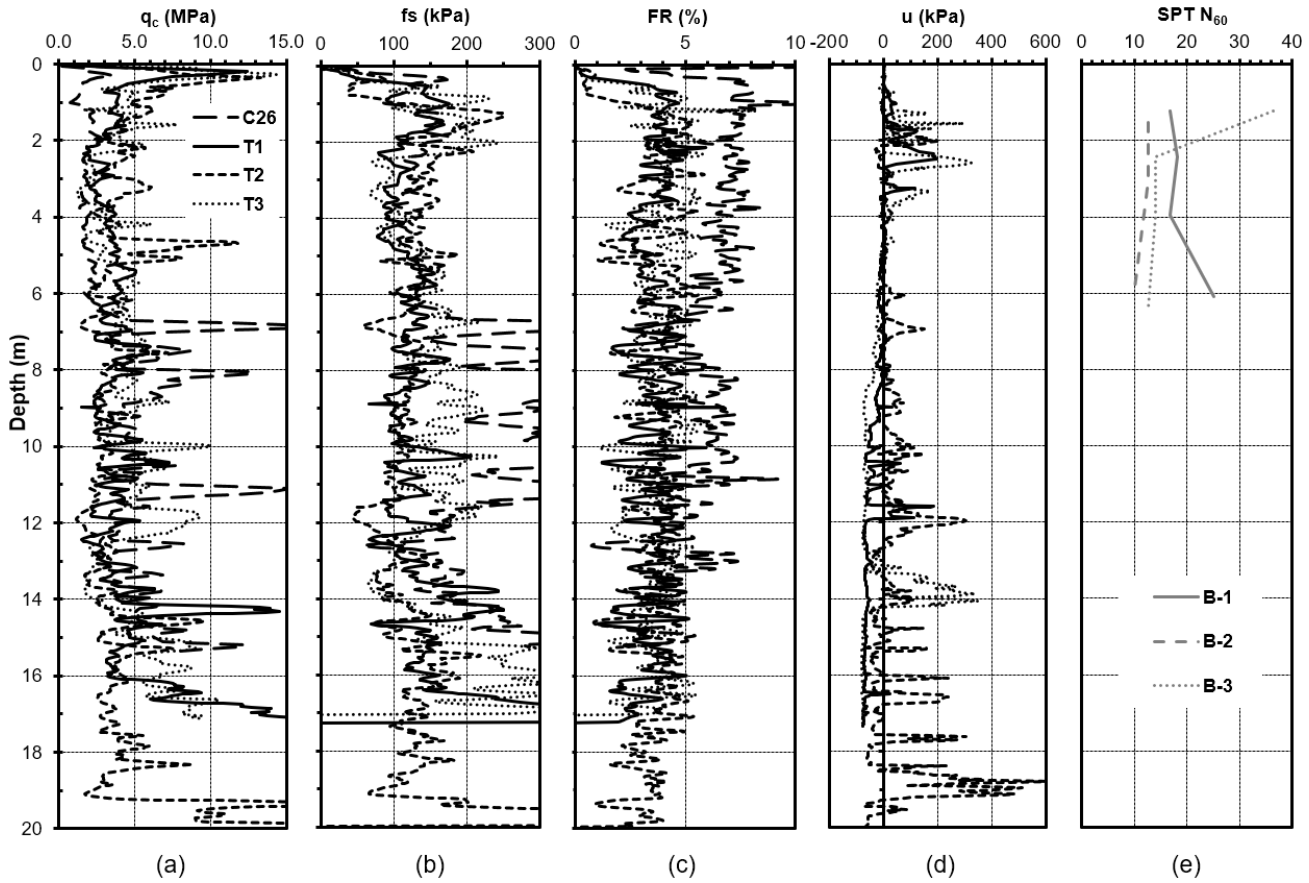

Figure 4. (a) tip resistance, q_c, (b) sleeve friction, f_s, (c) friction ratio, FR, (d) pore pressure, u, (e) SPT N_{60}.

3.2. Laboratory testing

The shear strength for the instrumented soil mass was estimated by the use of consolidated drained (CD) triaxial shear tests. Drained tests were selected because they most accurately represent the long-term strength of the soil. CD tests were performed on undisturbed Shelby tube samples in accordance with [4]. The results of the saturated, consolidated drained triaxial shear tests are summarized in Table 1.

Table 1. Shear strength with depth based on CD triaxial test results.

Depth (m)	Samples	Effective Friction, ϕ' (deg)	Effective Cohesion, c' (kPa)
0.0–2.4	1, 2, 3	17.0	23.6
2.4–4.6	4, 5, 6	31.9	16.1
4.6–6.1	7, 8, 9	28.4	20.4
6.1–7.8	10, 11, 12	23.3	32.2

Unsaturated triaxial shear tests were also performed on undisturbed Shelby tube samples that were collected during the geotechnical exploration. Procedures for the unsaturated triaxial shear tests were followed as presented in [5]. The results of the unsaturated triaxial shear tests are summarized in Figure 5. The results of the unsaturated tests showed that the samples that were tested at a suction of 69 kPa resulted in an increased cohesion of approximately 24.6 kPa over the saturated samples, indicating that apparent cohesion was present during the unsaturated tests. Based on this result, the unsaturated strength parameter (ϕ^b) was determined to be 19.6° for a matric suction range of 0 to 69 kPa when ϕ' was held constant.

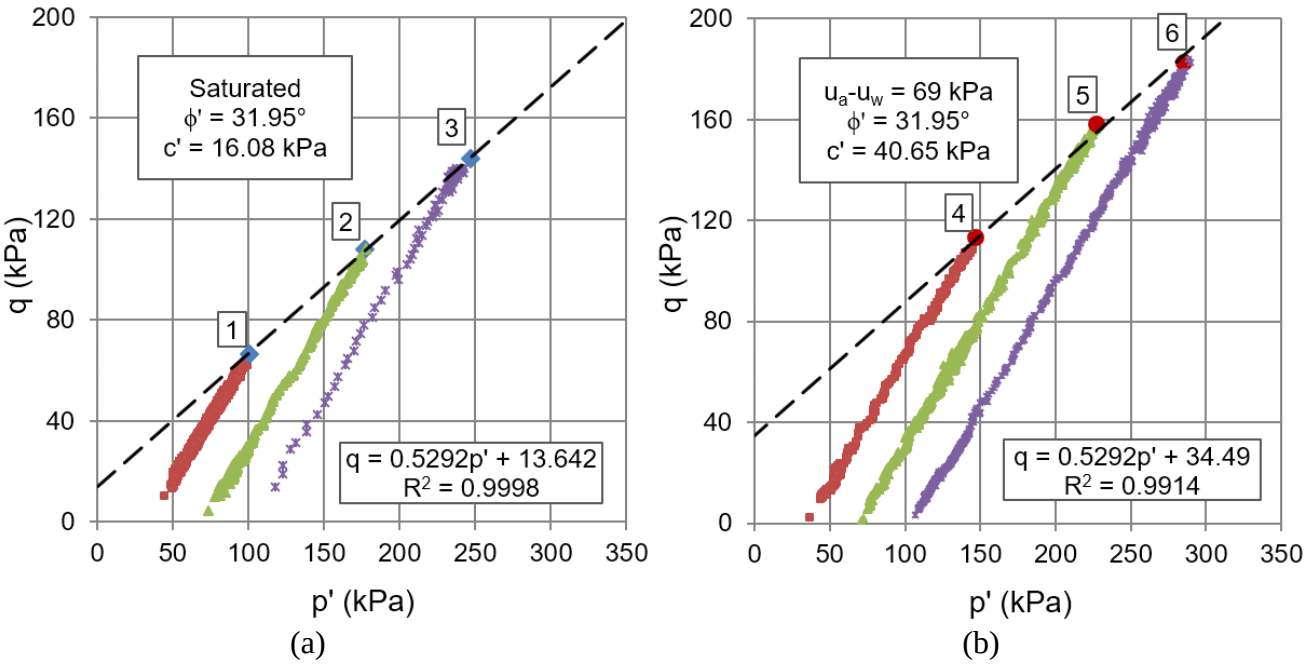

Figure 5. Failure criterion for (a) saturated samples and (b) unsaturated samples.

Permeability tests were performed on undisturbed samples taken from the excavation location to determine the seepage properties of the soil surrounding the excavation. The procedures for the permeability test followed those presented in [6]. The results of the permeability tests are summarized in Table 2.

Table 2. Permeability results.

Sample #	Sample Depth (m)	Hydraulic Gradient, i	Permeability, k (m/s)
1	0.0–2.4	4.6	1.3×10^{-5}
2	2.4–3.0	4.6	3.7×10^{-6}
4	3.0–4.6	4.6	1.2×10^{-5}
8	4.6–6.1	4.6	6.8×10^{-6}
11	6.1–7.8	4.6	2.1×10^{-7}

4. Results

4.1. Observational Results

The two test excavations were constructed in subsequent years and were both observed for a period of one year. The following general observations were made based on the outcome of the two excavations:

- The residual soil profile consisted of layers with variable properties. Thin granular layers were also observed (Figure 6) which caused a premature failure on the non-instrumented side of Excavation #1 during the excavating process.
- While excavating, tension cracks developed (almost immediately), which ran parallel to the face of the excavation approximately 1.5–2 m away from the face. Each failure plane observed intersected one of the excavation created tension cracks.
- Each failure occurred near a time of heavy rainfall, which implied that the reduction in apparent cohesion with increased soil moisture was a driving force for failure, as well as hydrostatic pressures within the tension crack.
- It appeared that most failures started at the bottom of the trench with some type of undermining caused by water entering the trench during a rain event, and eventually propagated to the surface approximately 1.5–2 m behind the excavation face (along the tension crack). The undermining that had occurred in Excavation #2 along the toe of the slope just before failure is shown in Figure 7.

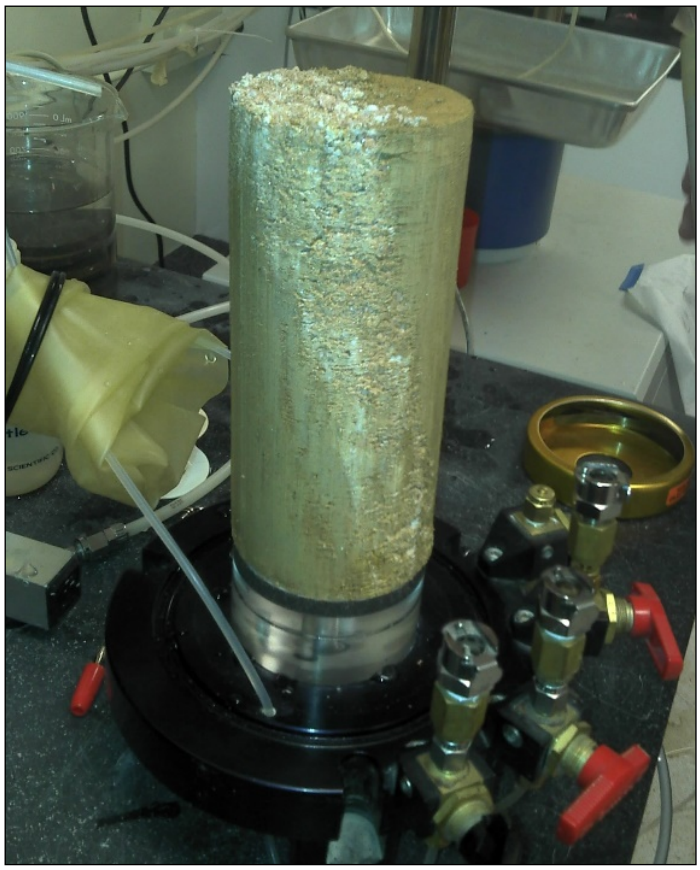

Figure 6. Thin layers present in undisturbed soil samples.

Figure 7. Undermining from water in bottom of trench.

Photos taken of Excavation #1 before and after failure are shown in Figure 8. Time-lapse photos of Excavation #2 before and after each failure are shown in Figure 9. An enlargement of Excavation #2 after the initial failure can be seen in Figure 10. Also, the progression of the tension cracks over time leading up to the time of failure can be seen in Figure 11. In general, the tension cracks started as small cracks, and grew larger over time, even in areas where failure had not occurred.

Figure 8. Excavation #1 before and after failure.

Figure 9. Excavation #2 time-lapse photos before and after failure.

Figure 10. Excavation #2 after initial failure on 9/21/11.

Figure 11. Tension crack progression over time (Excavation #1).

4.2. Sensor data

The measured displacements over time for the two test excavations are summarized in Figure 12. The pore pressure and precipitation measurements throughout the test period for Excavations #1 and #2 are shown in Figures 13 and 14 (respectively). A vertical line was drawn at the date and time of each failure for reference. The difference in the matric suction in the zone closest to the excavation (1.8 m) versus the zone that is further away from the excavation (4.6 m) is illustrated in Figure 13. The tension cracks that developed along the path of the front row of sensors allowed water to easily penetrate the soil, and therefore saturate to a greater depth than the soil further away from the excavation face. Because the matric suction values remained relatively stable in the soil further away from the excavation face, the presence of water in the tension cracks was determined to be a primary factor resulting in the failure of the excavations.

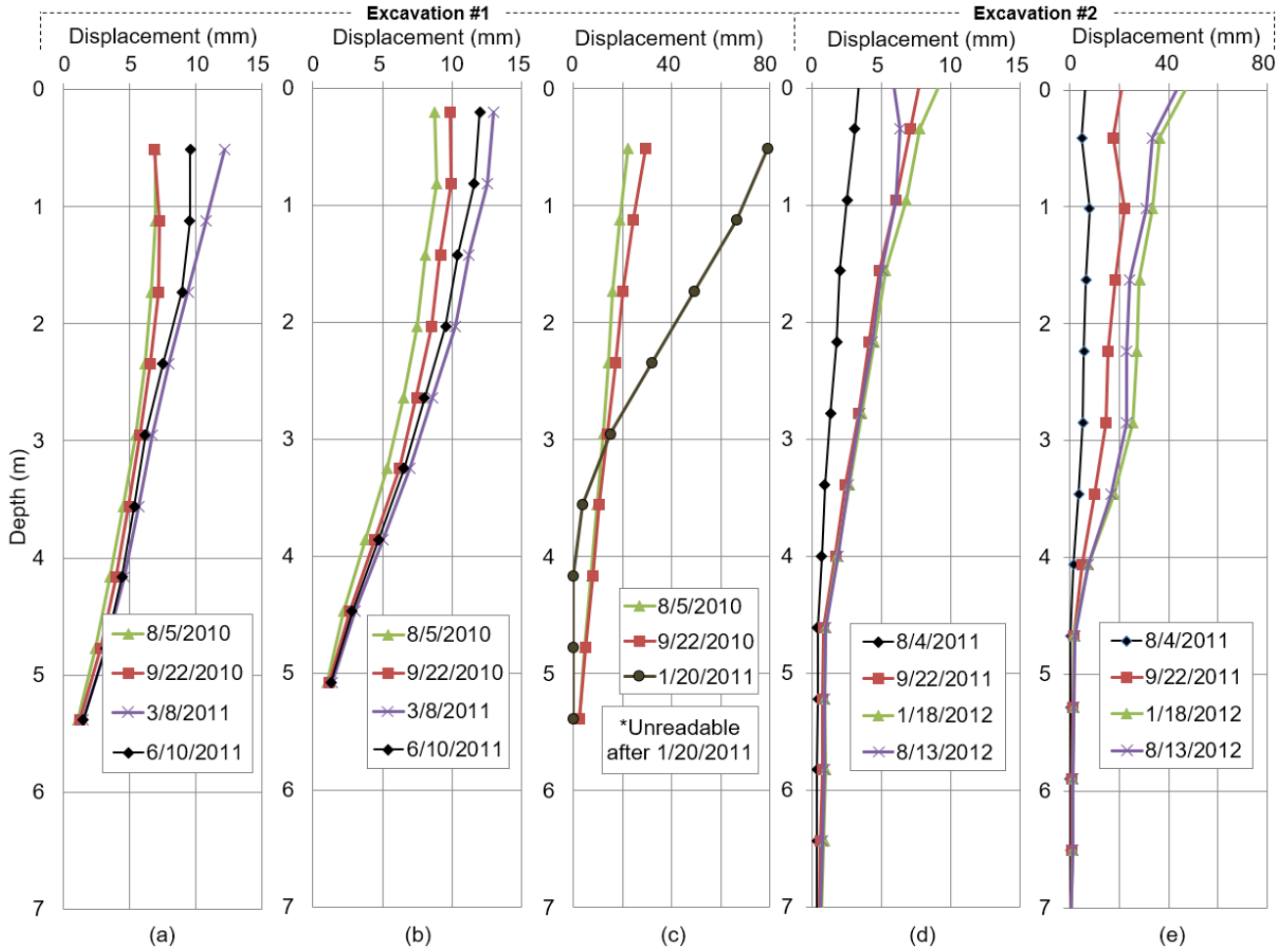

Figure 12. Inclinometer measured displacement data for (a) Southeast (4.3 m offset), (b) Northeast (4.3 m offset, (c) Northwest (1.8 m offset), (d) West (4.6 m offset), (e) East (1.8 m offset).

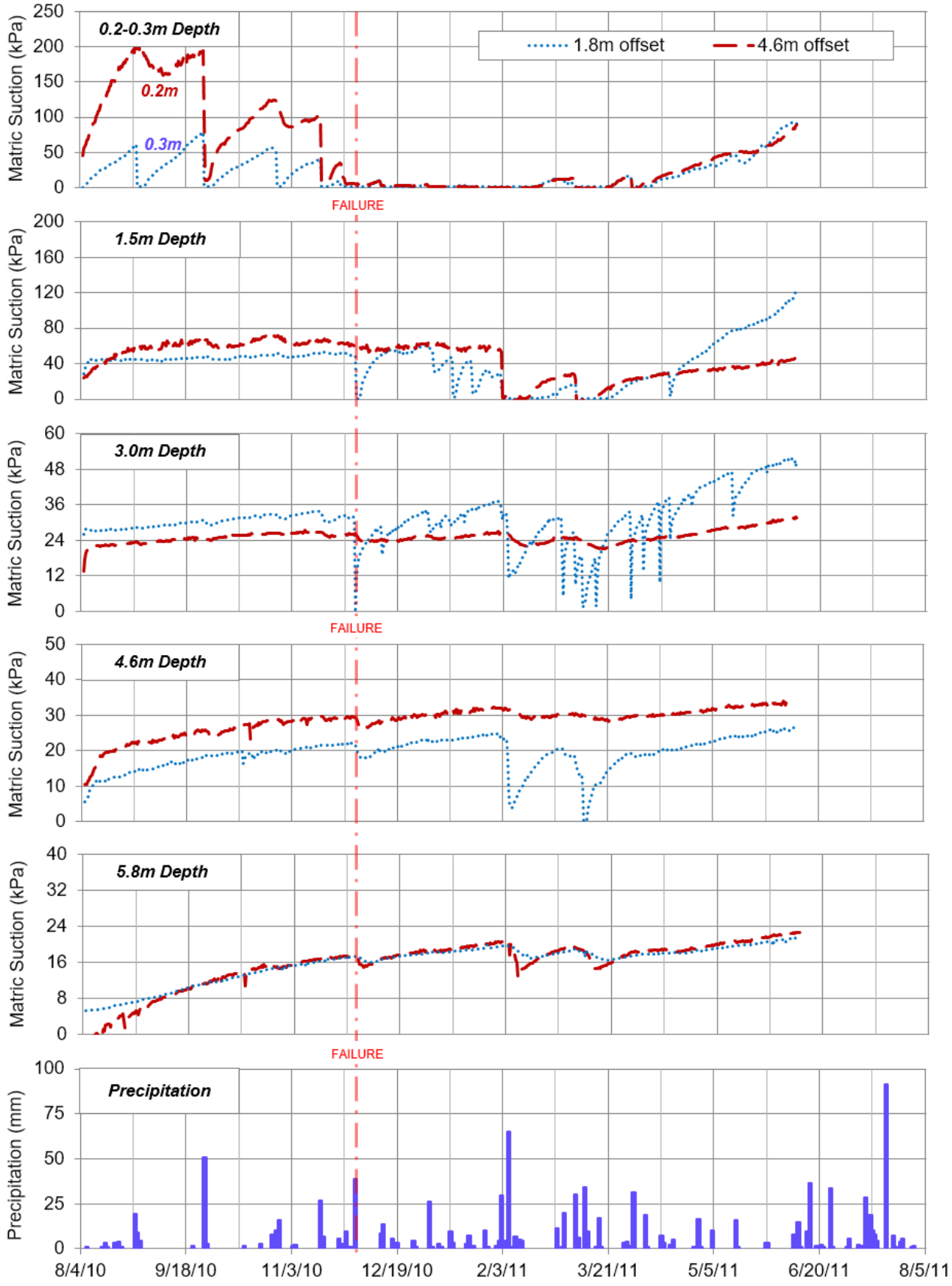

Figure 13. Matric suction and precipitation vs. time (Excavation #1).

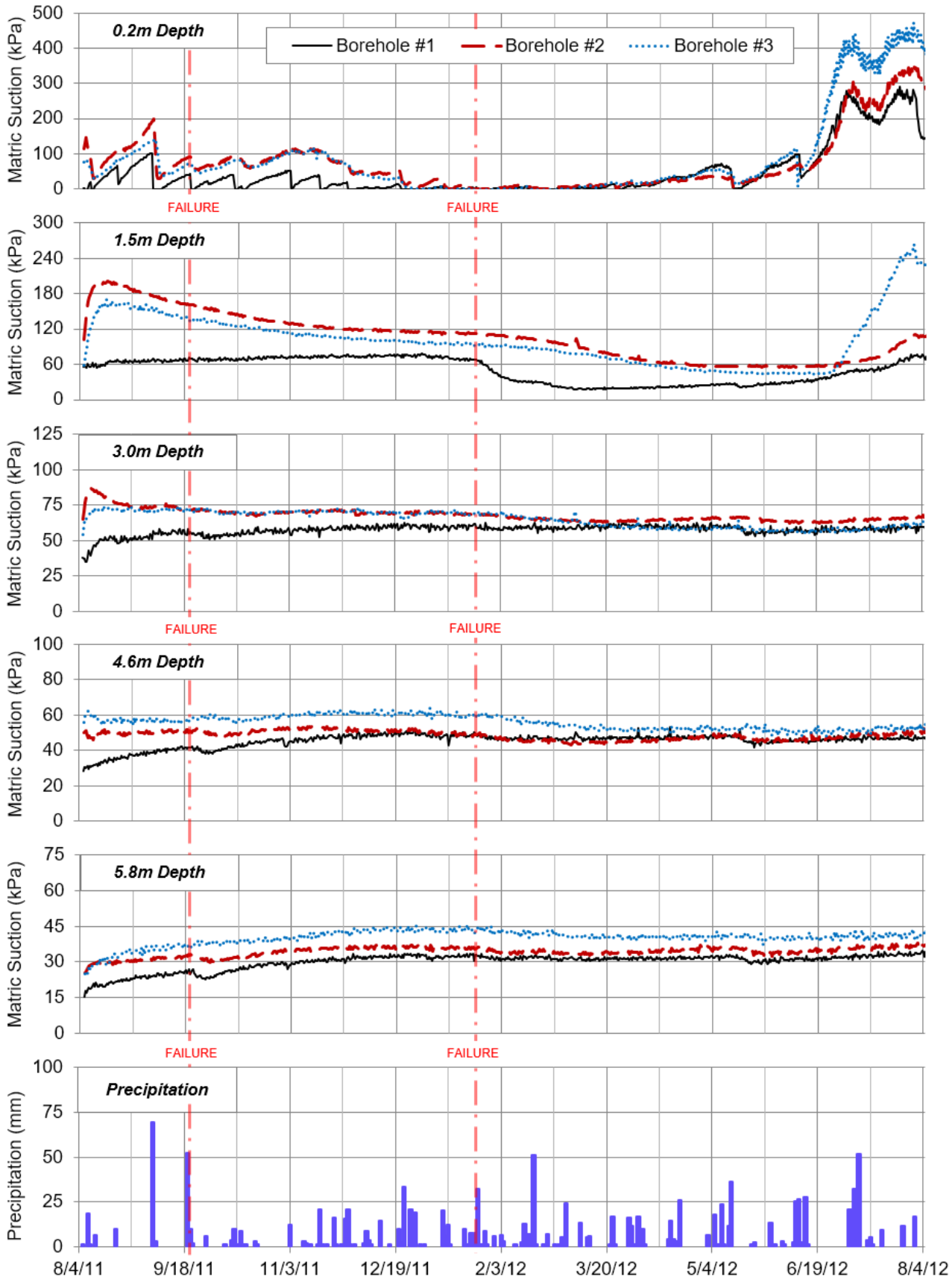

Figure 14. Matric suction and precipitation vs. time 4.6m offset (Excavation #2).

From the data in Figures 13 and 14, the following trends can be seen regarding the matric suction of the soil profile. Soils shallower in depth experienced a much higher fluctuation in matric suction when compared to deeper soils. Also, soils closer to the excavation face experienced much higher fluctuation in matric suction when compared to the soils farther away from the excavation face. This was likely influenced by the fact that the sensors closest to the excavation face were more closely aligned with the tension cracks which allowed water to penetrate the soil to a greater depth. Weather patterns, such as seasonal changes, droughts, etc. were also reflected in the matric suction data, particularly in the sensors closer to the ground surface. Also, the trend of decreased permeability with higher levels of matric suction was evident in several sensor locations, because soils with higher levels of matric suction tended to be influenced less by rain events when compared to soils near saturation.

5. Analysis

A finite element model was created based on the material properties and boundary conditions that were collected during the test period. The soil properties that used in the model are summarized in Table 3. The main goal of the model was to provide a connection between the characterized strength parameters of the soil, and the observational results in the field so that conclusions could be drawn based on the factors that were contributing to failure.

Table 3. Finite element model soil property summary.

Layer ID	Top Depth	Bottom Depth	Effective Friction (ϕ')	Effective Cohesion (c')	Effective Modulus (E')	Permeability at Saturation k (m/s)	Moist Unit Weight (γ)
NGES 0.2 m	0.0 m	0.8 m	17.0º	23.6 kPa	8750 kPa	1.3×10^{-5}	18.7 kN/m^3
NGES 1.5 m	0.8 m	2.2 m	17.0º	23.6 kPa	8350 kPa	1.3×10^{-5}	17.1 kN/m^3
NGES 3.0 m	2.2 m	3.8 m	31.9º	16.1 kPa	4350 kPa	3.7×10^{-6}	17.5 kN/m^3
NGES 4.6 m	3.8 m	5.2 m	28.4º	20.4 kPa	5350 kPa	1.2×10^{-5}	18.3 kN/m^3
NGES 5.8 m	5.2 m	30 m	23.3º	32.2 kPa	6100 kPa	6.8×10^{-6}	18.7 kN/m^3

The model consisted of a transient seepage model to approximate pore pressures along the failure plane at failure, along with a time-deformation analysis, and a finite element slope stability analysis. A schematic of the model geometry is shown in Figure 15.

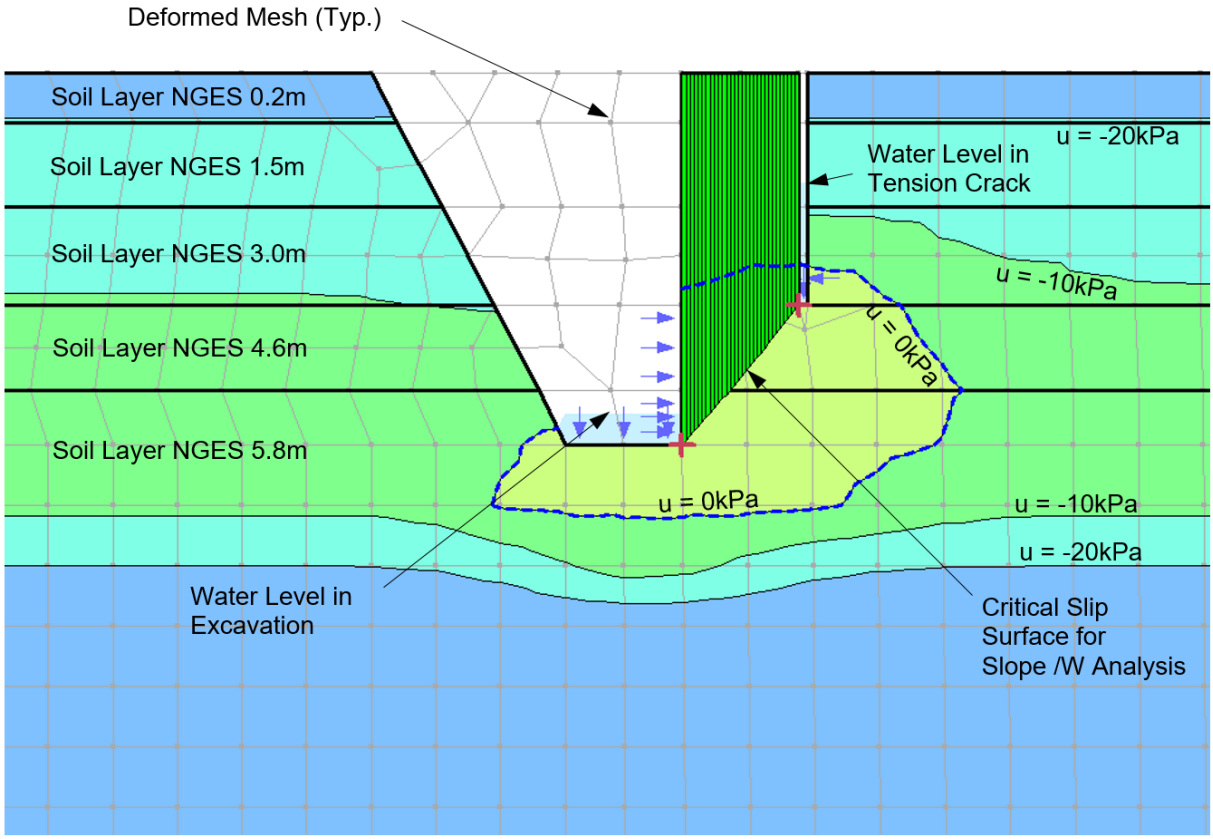

Figure 15. Slope stability analysis of the deformed mesh with modeled pore pressures after heavy rainfall.

Because it was evident that the failure was initiated by the increase in pore pressures due to a rain event, a sensitivity analysis was conducted to determine the impact that the water level in the tension crack had on the slope stability (since this was not able to be measured directly in the field). These results are summarized in Table 4.

A similar analysis was performed to determine how the matric suction impacted the factor of safety of the excavation. The calculated factors of safety for the matric suction measured by the sensors before and after heavy rainfall (at the critical state just before failure) are shown in Table 5.

Table 4. Calculated factors of safety for various water levels in tension crack.

Water Level in Tension Crack	Finite Element	Ordinary	Bishop	Janbu	Morgenstern Price
4.0 m	0.831	0.913	0.956	0.949	0.944
2.0 m	0.954	0.931	0.948	0.943	0.939
0.2 m	1.137	0.985	0.987	0.987	1.230
0.0 m	1.161	1.006	1.007	1.006	1.239

Table 5. Calculated factors of safety before and after heavy rainfall.

Matric Suction	Finite Element	Ordinary	Bishop	Janbu	Morgenstern Price
Dry Conditions	1.283	1.096	1.097	1.096	1.097
After Heavy Rainfall	0.954	0.931	0.948	0.943	0.939

A comparison between the finite element factor of safety, and the Mohr-Coulomb strength parameters for the soil is shown in Table 6. For this comparison, the boundary conditions were input into the model based on the collected data at the time of failure, and the tension crack was assumed to be half full. This table identifies the conservative nature of assuming c' = 0 for residual soils, as well as the danger of overestimating cohesion by including the apparent cohesion of unsaturated soils in the c' calculation.

Table 6. Mohr-Coulomb strength parameters vs. finite element factor of safety (critical state).

c' (kPa)	$\phi = 0^o$	$\phi = 20^o$	$\phi = 25^o$	$\phi = 30^o$	$\phi = 35^o$
0 kPa	--	--	--	0.53	0.62
10 kPa	0.42	0.67	0.67	0.76	0.80
20 kPa	0.79	0.81	0.84	0.93	1.03
30 kPa	1.04	1.02	1.09	1.19	1.32
40 kPa	1.13	1.28	1.37	1.46	1.56

6. Conclusions

6.1. Mode of failure

For this experiment, it was determined that the infiltration of rain water was the primary catalyst for failure, because it resulted in a decrease in matric suction in the layers that were not previously saturated. Since both excavations developed a tension crack almost immediately after excavation, and both eventually failed along that same tension crack, it was also concluded that the tension crack was an important factor impacting the stability of the excavations, because it provided a path for water to easily saturate the soil along the critical failure plane, and create hydrostatic pressure behind the soil mass with each significant rain event. Modeling results supported this theory, proving that the factor of safety for the excavation was approximately 0.3 higher in dry conditions than after a significant rain event, indicating a strong connection between matric suction and the stability of the excavation. However, there were some significant rain events in which failure did not occur which indicates that other factors were involved as well, such as the change in geometry due to the deformation of the soil mass at the time of failure, the overall moisture levels throughout the soil profile, etc. Also, the intensity of the rain events would also play a key role because a high intensity storm that generates higher amounts of runoff would create more hydrostatic pressure in the tension crack when compared to a lower intensity rain event, even if the total rainfall is the same.

6.2. Residual soil strength properties

The modeling results support the theory that residual soil behaves as a c-ϕ soil having both frictional and cohesive properties. However, thin layers of materials with little cohesion were also identified, which could cause localized slope stability failures, especially when oriented along a potential slip surface.

The results of the finite element analysis concluded that the c' and ϕ' values determined by consolidated-drained triaxial testing were reasonably accurate for modeling the behavior of residual soil. However, because of the heterogeneous nature of residual soil, high quantities of tests may be

necessary to accurately define the layers and identify any weak layers, which could make this type of testing unfeasible for many projects.

While reducing triaxial data, it was realized that care must be taken when determining the triaxial ϕ' and c' as to not overestimate the cohesive component. Forcing a linear trendline to a p'-q diagram may have a tendency to overestimate the value for cohesion because the Mohr-Coulomb failure envelope is non-linear [7]. This is especially true when forcing a linear trendline using only tests at higher effective confining stresses, therefore it is critical that effective stresses in laboratory tests bound the effective stresses that are seen in the field. The finite element model predicted an increase in the factor of safety by magnitudes as great as 0.3 when fitting a linear trendline to tests with confining stresses greater than or equal to 70 kPa. The impact that increased values of cohesion has on the factor of safety was previously illustrated in Table 6.

6.3. Unsaturated soil properties

Based on modeling results, it was determined that the apparent cohesion caused by negative pore pressure in unsaturated soil can greatly influence the factor of safety of the excavation, illustrating the importance of characterizing the soil in such a manner that this apparent cohesion can be determined separate from the saturated effective cohesion of the soil. Mistakenly using the unsaturated cohesion in a situation where the soil is susceptible to changes in moisture may lead to failure as the soil nears saturation.

Sufficient evidence exists in published literature to indicate that negative pore pressures may remain relatively constant depending on the permeability of the soil, and the rate at which water can infiltrate. The data collected in these tests support this theory and showed relatively stable pore pressures at greater depths where tension cracks were not present, even with heavy rainfall. Because of this, certain geotechnical designs may be modified to benefit from the apparent cohesion caused by matric suction. Zhang et al. [8] performed a numerical study on an unsaturated slope, and proved that under certain conditions, matric suction was maintained. Zhang et al. [8] also proposed that ground cover may be utilized to further stabilize the levels of suction and emphasized the need for engineers to address more appropriate design assumptions related to the permanence of matric suction. The results of this experiment also support this recommendation and proved that, significant strength can be provided by matric suction as long as pore pressures can be maintained.

6.4. Unsaturated residual soil characterization

When determining c’ and ϕ' for use in geotechnical design, care must be taken to exclude the apparent cohesion created by matric suction in design calculations. Many widely used insitu test methods such as the SPT and CPT, are not capable of determining the portion of the strength that is attributed to negative pore pressures, and therefore, the results of these tests can vary significantly depending on seasonal changes in the moisture content of the soil. In designs where these soil parameters are critical, and where it is probable that soil moisture conditions will change over time, it is recommended that these parameters be obtained by testing saturated samples in the laboratory.

Because of the heterogeneous nature of residual soil, thin layers of weak or cohesionless material may also be present which may result in a significant decrease in the factor of safety.

Therefore, it is also recommended that the testing program be suitable for identifying such weak layers, to ensure that the strength parameters obtained from testing truly reflect the critical state.

Acknowledgements

The authors acknowledge Neill Belk and Jonathan Honeycutt for assistance with site investigation and field work. Funding for this project was provided by the United States Federal Highway Administration through an Eisenhower Research Fellowship. Additional resources were provided by the Auburn University Highway Research Center and the University of North Carolina Charlotte Department of Civil and Environmental Engineering.

Conflicts of interest

All authors declare no conflicts of interest in this paper.

References

1. ASTM Standard D 5298-10 (2010) Standard Test Method for Measurement of Soil Potential (Suction) Using Filter Paper, Annual Book of ASTM Standards, ASTM International, West Conshohocken, PA.
2. Pictometry International Corp (2012) Springvilla, AL. Available from: http://www.bing.com/mapspreview?&cp=pdz5107wrpbz&lvl=20&style=b&v=2&sV=1&form=S00027.
3. Vinson JL, Brown DA (1997) *Site Characterization of the Spring Villa Geotechnical Test Site and a Comparison of Strength and Stiffness Parameters for a Piedmont Residual Soil*. Report No. IR-97-04, Highway Research Center, Harbert Engineering Center, Auburn University, AL.
4. ASTM Standard D 7181-11 (2011) Standard Test Method for Consolidated Drained Triaxial Compression Test for Soils, Annual Book of ASTM Standards, ASTM International, West Conshohocken, PA.
5. Burrage RE, Anderson JB, Pando MA, et al. (2011) A cost effective triaxial test method for unsaturated soils. *Geotech Test J* 35: 50–59.
6. ASTM Standard D 5084-00 (2000) Standard Test Methods for Measurement of Hydraulic Conductivity of Saturated Porous Materials Using a Flexible Wall Permeameter, Annual Book of ASTM Standards, ASTM International, West Conshohocken, PA.
7. Lambe TW, Whitman RV (1969) *Soil Mechanics*. John Wiley and Sons, New York.
8. Zhang LL, Fredlund DG, Zhang LM, et al. (2004) Numerical study of soil conditions under which matric suction can be maintained. *Can Geotech J* 41: 569–582.

AIMS Press